JCTC Journal of Chemical Theory and Computation

Density Functional Study of 2-[(R-Phenyl)amine]-1,4-naphthalenediones†

Z. Gómez-Sandoval,‡ P. Calaminici,‡ A. M. Köster,*,‡ B. Lotina-Hennsen,§ B. King-Díaz,§ N. Macías-Ruvalcaba,§ M. Aguilar-Martínez,§ and M. Jiménez-Estrada||

Departamento de Química, CINVESTAV, Avenida Instituto Politécnico Nacional 2508, A.P. 14-740 México D.F. 07000, México, Facultad de Química, Departamentos de Bioquímica y Fisicoquímica, Universidad Nacional Autónoma de México, Ciudad Universitaria, México D.F. 04510, México, and Instituto de Química, Universidad Nacional Autónoma de México, Ciudad Universitaria, México D.F. 04510, México.

Received November 12, 2006

Abstract: The molecular and electronic structures of a series of 2-[(R-phenyl)amine]-1,4-naphthalenediones (R = m-Me, p-Me, m-Et, p-CF_3, p-Hex, p-Et, m-F, m-Cl, p-OMe, p-COMe, p-Bu, m-COOH, p-Cl, p-COOH, p-Br, m-NO_2, m-CN, and p-NO_2) and their anions are investigated in the framework of density functional theory. The calculations are of all-electron type using a double zeta valence polarization basis set optimized for density functional theory methods. The theoretical study shows that all compounds are nonplanar. The nonplanarity can be rationalized in terms of occupied π orbitals. A linear correlation between the measured half-wave potentials and the calculated gas-phase electron affinities is found. It holds for local as well as generalized gradient corrected functionals. Structural parameters, harmonic vibrational frequencies, and adiabatic and vertical electron affinities as well as orbital and spin density plots of the studied compounds are presented.

I. Introduction

The quinone moiety appears in a wide range of natural compounds including the electron transport chain of bacteria, mitochondria, and chloroplasts.[1] Interruption of the electron transport chain is an attractive avenue toward green, i.e., ecological less disastrous, herbicides. Therefore, many studies have focused on the chemistry and toxicology of quinone compounds. The biological activity of quinones[2] is based on their redox system which permits the formation of anion radicals ($Q^{\bullet -}$) and dianions (Q^{2-}) under mild conditions.[3] These species are capable of interaction with cellular compounds such as oxygen, deoxyribo nucleic acid (DNA), and proteins, modifying their biological activities.[4] The ability of quinones to accept electrons depends on their chemical structure[5] and the microenvironment of the reaction.[6] The biological activity of quinones can be modified by substituting the quinone system.[7,8] Such substitutions do not alter the general characteristic of the quinone redox system but change in a systematic way its electrochemical behavior. In fact, the use of a heteroatom which allows a gradual modulation between the quinone and a substituted phenyl has been suggested in the literature.[9,10] In this sense, 1,4-naphthoquinone compounds and their derivatives have been widely studied due to their pharmacological use as agents against tuberculosis,[11] malaria,[12] bacterial infections,[13] and neoplasia growth,[14] as larvicides,[15] molluscicides,[15] herbicides,[16] and fungicides.[17]

Numerically the substituent effects can be described by molecular properties that are sensitive to the substituent.[18,19] Because a number of naturally occurring quinones play an important role in electron transport the quinone-hydroxy quinone redox couples are intensive studied. The measured

† Dedicated to Professor Dennis R. Salahub on the occasion of his 60th birthday.

* Corresponding author e-mail: akoster@cinvestav.mx.

‡ CINVESTAV.

§ Departamentos de Bioquímica y Fisicoquímica, Universidad Nacional Autónoma de México.

|| Instituto de Química, Universidad Nacional Autónoma de México.

10.1021/ct6003356 CCC: $37.00
Published on Web 04/03/2007

half-wave potentials are sensitive to the substituent pattern and are, therefore, well suited for a numerically description of substituent effects. With this in mind a group of 2-[(R-phenyl)amine]-1,4-naphthalenediones (PANs) have been investigated in our laboratory,[20] recently. The half-wave potentials (HWPs) of these compounds were measured by cyclic voltametry in acetonitrile at room temperature. As supporting electrolyte 0.1 M tetraethylammonium tetrafluoroborate was used. Under these conditions ion pairing is minor with anion radicals,[21,22] and, therefore, solvent effects for the first electron-transfer reaction are negligible.[23] As a consequence, the measured HWPs for the first one-electron transfer, corresponding to the formation of the radical anions, can be directly compared with theoretical gas-phase studies.

Quantitative structure−activity relationship (QSAR) analysis between the herbicide activity and various molecular properties of the studied PAN compounds[20] reveal that the HWPs for the first one-electron transfer and detailed geometrical structure data are main ingredients for the prediction of the biological activity of PAN derivatives.[24] Therefore, the reliable theoretical prediction of these molecular properties enables the rational design of new herbicides based on this compound class.

With this goal in mind, the results of a density functional theory (DFT) study of a series of PAN derivatives (neutral and anionic) are presented. Optimized structure parameters, harmonic vibrational frequencies, and orbital and spin density plots as well as calculated adiabatic and vertical electron affinities are presented. The relation between the geometric and electronic structure is discussed in details. It is shown that Hückels π counting rule[25] can be used to rationalize the geometric structure of the neutral and anionic PAN derivatives.

The article is organized as follows. In section II the computational method is described. In section III the obtained results are analyzed. Finally, in section IV, the conclusions are summarized.

II. Computational Details

Full geometry optimizations, without symmetry constraints, for the following 19 neutral and anionic compounds, H PAN, m-Me PAN, p-Me PAN, m-Et PAN, p-CF_3PAN, p-Hex PAN, p-Et PAN, m-F PAN, m-Cl PAN, p-OMe PAN, p-COMe PAN, p-Bu PAN, m-COOH PAN, p-Cl PAN, p-COOH PAN, p-Br PAN, m-NO_2 PAN, m-CN PAN. and p-NO_2 PAN, were performed. The structures of some selected dianionic compounds such as H, p-Cl, m-Cl, p-Me, and m-Me PAN, were optimized, too.

The optimizations were performed within the density functional theory framework as implemented in the program deMon2k.[26] Local and gradient corrected exchange-correlation functionals were used. For the local calculations the Dirac exchange[27] in combination with the correlation functional proposed by Vosko, Wilk, and Nusair (VWN)[28] was employed. The gradient corrected calculations were performed with the generalized gradient approximation (GGA) for the exchange proposed by Becke[29] and the correlation approximation of Lee, Yang and Parr (BLYP).[30] The calculations were of all-electron type using a DFT optimized

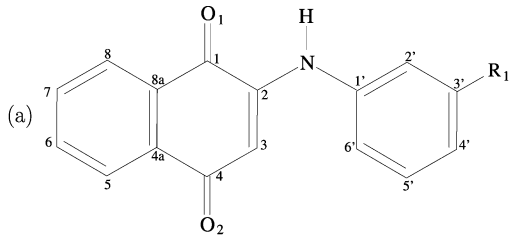

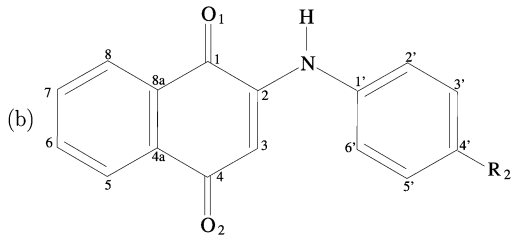

Figure 1. Structure and atomic labels of *meta*- (a) and *para*-(b) substituted PAN derivatives.

double ζ split valence plus polarization basis set (DZVP), and an A2 auxiliary function set[31] for the variational fitting of the Coulomb potential.[32]

A quasi-Newton Levenberg-Marquard method, employing internal redundant coordinates with analytic energy gradients, was used for the structure optimization.[33] The convergence was based on the Cartesian gradient and displacement vectors with thresholds of 10^{-4} and 10^{-3} au, respectively. In order to verify that the optimized structures are minima on the potential energy surface (PES) harmonic frequencies were calculated for selected compounds. The second derivatives were obtained by numerical differentiation (two-points finite difference) of the analytic energy gradients using a displacement of 0.001 au from the optimized geometry for all 3N coordinates. The harmonic frequencies were then obtained by diagonalizing the mass-weighted Cartesian force constant matrix.

III. Results and Discussion

III-A. Structural Analysis. The structures and atomic labels of the studied PAN compounds are shown in Figure 1a,b. R_1 and R_2 represent the substituents in the *meta* and *para* positions, respectively. The optimized VWN geometries are listed in Tables 1−3. Because the DZVP basis set is parametrized for the local VWN functional the optimized structure parameters are usually reliable within 1−2 pm and 1−2 degrees for organic compounds.[34] Our DFT calculations show that all neutral PANs are nonplanar independently from the functional used in the optimization. This result is in disagreement with a previous theoretical study[35] in which planarity was enforced by the optimization strategy. If this restriction is released,[36] then nonplanar structures are also obtained with the theoretical approach in ref 35.

The $C_2-N-C_{1'}-C_{6'}$ dihedral angle (Table 1) for the neutral PANs is found in a range between 14 and 20 degrees. These results were obtained from the optimization of several different initial geometries with varying start values for the

Table 1. Structure Data of the Optimized Neutral PANs[a]

geometrical parameter	p-Me	p-CF_3	p-Hex	p-Et	p-OMe	p-COMe	geometrical parameter	p-Me	p-CF_3	p-Hex	p-Et	p-OMe	p-COMe
C_1-O_1	1.238	1.238	1.238	1.238	1.239	1.238	$O_1-C_1-C_2$	118.6	118.3	118.6	118.6	118.6	118.3
C_1-C_2	1.496	1.497	1.496	1.496	1.494	1.497	$C_1-C_2-C_3$	120.6	120.5	120.6	120.6	120.6	120.5
C_2-C_3	1.374	1.370	1.374	1.373	1.375	1.370	C_1-C_2-N	109.6	109.3	109.7	109.6	109.6	109.4
C_3-C_4	1.439	1.443	1.439	1.439	1.437	1.443	C_2-N-H	109.4	109.1	109.4	109.4	109.4	109.1
C_4-O_2	1.242	1.240	1.242	1.242	1.243	1.240	$C_2-N-C_{1'}$	132.1	132.2	132.1	132.1	132.0	132.5
C_4-C_{4a}	1.488	1.487	1.488	1.488	1.488	1.486	C_2-C_3-C_4	121.8	121.7	121.8	121.8	121.8	121.8
$C_{4a}-C_5$	1.390	1.390	1.390	1.390	1.391	1.390	$H-N-C_{1'}$	118.5	118.7	118.5	118.5	118.6	118.4
C_5-C_6	1.393	1.393	1.392	1.392	1.392	1.392	$C_{1'}-C_{2'}-C_{3'}$	120.8	120.8	120.7	120.7	121.1	120.7
C_6-C_7	1.398	1.398	1.398	1.398	1.398	1.398	$C_{1'}-C_{6'}-C_{5'}$	120.0	120.0	119.9	119.9	120.7	119.8
C_7-C_8	1.389	1.389	1.389	1.389	1.389	1.389	$C_{8a}-C_1-C_2$	118.5	118.6	118.5	118.5	118.4	118.6
C_8-C_{8a}	1.397	1.397	1.397	1.397	1.397	1.396	$C_2-N-C_{1'}-C_{2'}$	−163.4	−165.3	163.4	163.5	162.9	166.6
$C_{4a}-C_{8a}$	1.403	1.403	1.403	1.403	1.403	1.403	$O_1-C_1-C_2-N$	−0.6	−0.6	0.5	0.4	0.3	0.7
C_2-N	1.349	1.353	1.349	1.349	1.349	1.353	$H-N-C_2-C_1$	3.2	3.4	−3.3	−3.2	−2.9	−3.5
$N-H$	1.041	1.042	1.040	1.041	1.041	1.042	$C_1-C_2-C_3$-C_4	1.5	1.8	−1.5	−1.6	−1.3	−1.9
$N-C_{1'}$	1.386	1.381	1.386	1.386	1.387	1.380	C_2-C_3-C_4-C_{4a}	0.4	0.3	−0.5	−0.4	−0.5	−0.2
$C_{1'}-C_{2'}$	1.403	1.405	1.404	1.404	1.407	1.409	$C_2-C_1-C_{8a}-C_8$	−179.0	−178.8	178.9	178.9	179.0	178.8
$C_{2'}-C_{3'}$	1.386	1.383	1.386	1.386	1.380	1.379	$C_{8a}-C_1-C_2-N$	179.8	179.6	−179.6	−179.7	−179.8	−179.5
$C_{3'}-C_{4'}$	1.400	1.395	1.400	1.400	1.402	1.402	$C_1-C_2-N-C_{1'}$	−176.6	−175.6	176.4	176.5	176.5	175.5
$C_{4'}-R$	1.494	1.490	1.495	1.496	1.352	1.480	$O_1-C_2-C_4-O_2$	−173.3	−176.5	176.4	176.2	176.6	176.6
$C_{1'}-C_{6'}$	1.402	1.404	1.402	1.402	1.399	1.404	$C_2-N-C_{1'}-C_{6'}$	19.7	17.6	−19.9	−19.6	−19.8	−15.9
$C_{6'}-C_{5'}$	1.390	1.388	1.390	1.390	1.392	1.387	$O_1-H(N)$	1.926	1.910	1.927	1.927	1.925	1.912
$C_{5'}-C_{4'}$	1.398	1.393	1.397	1.397	1.397	1.399							

geometrical parameter	p-Bu	p-Cl	p-COOH	p-Br	p-NO2	PAN	geometrical parameter	p-Bu	p-Cl	p-COOH	p-Br	p-NO2	PAN
C_1-O_1	1.238	1.238	1.238	1.238	1.238	1.238	$O_1-C_1-C_2$	118.6	118.4	118.3	118.4	118.2	118.5
C_1-C_2	1.496	1.496	1.497	1.496	1.498	1.496	$C_1-C_2-C_3$	120.6	120.6	120.5	120.6	120.6	120.5
C_2-C_3	1.374	1.372	1.370	1.372	1.368	1.373	C_1-C_2-N	109.6	109.5	109.3	109.5	109.2	109.5
C_3-C_4	1.439	1.441	1.443	1.441	1.446	1.440	C_2-N-H	109.4	109.2	109.1	109.2	108.8	109.4
C_4-O_2	1.242	1.241	1.240	1.241	1.239	1.242	$C_2-N-C_{1'}$	132.1	132.0	132.5	132.1	132.6	132.2
C_4-C_{4a}	1.488	1.487	1.486	1.487	1.485	1.488	C_2-C_3-C_4	121.8	120.6	121.7	121.8	121.7	121.8
$C_{4a}-C_5$	1.390	1.390	1.390	1.390	1.390	1.390	$H-N-C_{1'}$	118.4	118.7	118.4	118.7	118.6	118.4
C_5-C_6	1.392	1.393	1.393	1.393	1.393	1.393	$C_{1'}-C_{2'}-C_{3'}$	120.7	121.1	120.6	121.2	120.8	120.8
C_6-C_7	1.398	1.398	1.398	1.398	1.398	1.398	$C_{1'}-C_{6'}-C_{5'}$	119.9	120.4	120.0	120.5	120.0	120.1
C_7-C_8	1.389	1.389	1.389	1.389	1.389	1.389	$C_{8a}-C_1-C_2$	118.5	118.5	118.6	118.5	118.6	118.5
C_8-C_{8a}	1.397	1.397	1.397	1.397	1.397	1.397	$C_2-N-C_{1'}-C_{2'}$	−162.9	163.9	166.3	164.7	167.5	163.4
$C_{4a}-C_{8a}$	1.403	1.403	1.403	1.403	1.403	1.403	$O_1-C_1-C_2-N$	−0.3	0.5	0.6	0.6	0.7	0.6
C_2-N	1.349	1.351	1.353	1.351	1.356	1.350	$H-N-C_2-C_1$	3.0	−3.2	−3.5	−3.3	−3.6	−3.4
$N-H$	1.041	1.041	1.042	1.041	1.043	1.041	$C_1-C_2-C_3$-C_4	1.5	−1.6	−1.9	−1.7	−2.0	−1.7
$N-C_{1'}$	1.387	1.384	1.380	1.383	1.376	1.386	C_2-C_3-C_4-C_{4a}	0.3	−0.4	−0.2	−0.3	−0.2	−0.4
$C_{1'}-C_{2'}$	1.404	1.404	1.408	1.404	1.409	1.404	$C_2-C_1-C_{8a}-C_8$	−179.2	178.9	178.7	178.8	178.7	178.8
$C_{2'}-C_{3'}$	1.385	1.385	1.380	1.386	1.380	1.387	$C_{8a}-C_1-C_2-N$	180.0	−179.6	−179.6	−179.5	−179.4	−179.5
$C_{3'}-C_{4'}$	1.400	1.394	1.400	1.393	1.394	1.396	$C_1-C_2-N-C_{1'}$	−176.8	175.9	175.4	175.6	174.6	176.5
$C_{4'}-R$	1.495	1.732	1.468	1.887	1.447	1.098	$O_1-C_2-C_4-O_2$	−176.5	176.6	176.5	176.5	176.5	176.5
$C_{1'}-C_{6'}$	1.401	1.402	1.405	1.403	1.406	1.402	$C_2-N-C_{1'}-C_{6'}$	19.1	−18.8	−16.5	−18.2	−14.8	−19.4
$C_{6'}-C_{5'}$	1.390	1.389	1.386	1.390	1.385	1.391	$O_1-H(N)$	1.926	1.917	1.911	1.916	1.900	1.923
$C_{5'}-C_{4'}$	1.397	1.392	1.398	1.390	1.391	1.393							

geometrical parameter	m-Me	m-Et	m-Cl	m-COOH	m−F	m-NO2	m-CN	geometrical parameter	m-Me	m-Et	m-Cl	m-COOH	m−F	m-NO2	m-CN
C_1-O_1	1.238	1.238	1.238	1.237	1.238	1.237	1.238	$O_1-C_1-C_2$	118.5	118.5	118.4	118.4	118.4	118.2	118.2
C_1-C_2	1.496	1.496	1.497	1.497	1.497	1.498	1.498	$C_1-C_2-C_3$	120.5	120.5	120.6	120.5	120.6	120.5	120.5
C_2-C_3	1.373	1.373	1.371	1.371	1.371	1.369	1.370	C_1-C_2-N	109.6	109.6	109.5	109.5	109.5	109.3	109.3
C_3-C_4	1.439	1.439	1.442	1.442	1.442	1.444	1.443	C_2-N-H	109.4	109.4	109.3	109.5	109.3	109.2	109.1
C_4-O_2	1.242	1.242	1.241	1.241	1.241	1.240	1.240	$C_2-N-C_{1'}$	132.2	132.3	132.0	132.0	131.9	131.9	132.0
C_4-C_{4a}	1.488	1.488	1.487	1.487	1.487	1.486	1.486	C_2-C_3-C_4	121.8	121.8	121.8	121.8	121.8	121.7	121.7
$C_{4a}-C_5$	1.390	1.390	1.390	1.390	1.390	1.390	1.390	$H-N-C_{1'}$	118.4	118.3	118.7	118.5	118.8	118.9	118.8
C_5-C_6	1.393	1.393	1.393	1.393	1.393	1.393	1.393	$C_{1'}-C_{2'}-C_{3'}$	121.8	121.7	120.0	120.5	119.3	119.4	120.5
C_6-C_7	1.398	1.398	1.398	1.398	1.398	1.398	1.398	$C_{1'}-C_{6'}-C_{5'}$	119.3	119.4	119.7	120.4	120.0	120.6	120.4
C_7-C_8	1.390	1.389	1.390	1.390	1.389	1.390	1.389	$C_{8a}-C_1-C_2$	118.5	118.5	118.5	118.5	118.5	118.6	118.6
C_8-C_{8a}	1.397	1.397	1.397	1.397	1.397	1.396	1.397	$C_2-N-C_{1'}-C_{2'}$	−163.5	164.1	−163.5	−163.6	162.6	−164.0	164.3
$C_{4a}-C_{8a}$	1.403	1.403	1.403	1.403	1.403	1.403	1.403	$O_1-C_1-C_2-N$	−0.7	0.7	−0.7	−0.7	0.7	−0.7	0.7
C_2-N	1.350	1.350	1.351	1.351	1.352	1.353	1.353	$H-N-C_2-C_1$	3.4	−3.3	3.5	3.7	−3.5	3.6	−3.4
$N-H$	1.040	1.040	1.041	1.041	1.041	1.041	1.041	$C_1-C_2-C_3$-C_4	1.7	−1.7	1.8	1.8	−1.8	1.8	−1.8
$N-C_{1'}$	1.386	1.386	1.384	1.385	1.385	1.382	1.382	C_2-C_3-C_4-C_{4a}	0.4	−0.4	0.3	0.3	−0.4	0.3	−0.3
$C_{1'}-C_{2'}$	1.403	1.403	1.403	1.399	1.403	1.400	1.400	$C_2-C_1-C_{8a}-C_8$	−178.8	178.8	−178.8	−178.8	178.8	−178.8	178.8
$C_{2'}-C_{3'}$	1.391	1.390	1.386	1.390	1.383	1.384	1.396	$C_{8a}-C_1-C_2-N$	179.4	−179.4	179.5	179.5	−179.5	179.6	−179.5
$C_{3'}-C_{4'}$	1.401	1.401	1.394	1.399	1.390	1.391	1.404	$C_1-C_2-N-C_{1'}$	−176.6	176.3	−176.0	−175.8	176.3	−175.8	175.6
$C_{3'}-R$	1.495	1.498	1.733	1.476	1.340	1.460	1.425	$O_1-C_2-C_4-O_2$	−176.4	176.4	−176.4	−176.5	176.3	−176.5	176.6
$C_{1'}-C_{6'}$	1.401	1.401	1.402	1.404	1.403	1.405	1.404	$C_2-N-C_{1'}-C_{6'}$	19.1	−18.6	18.8	19.1	−20.1	18.5	−18.2
$C_{6'}-C_{5'}$	1.391	1.391	1.390	1.391	1.391	1.391	1.391	$O_1-H(N)$	1.926	1.926	1.918	1.924	1.920	1.911	1.910
$C_{5'}-C_{4'}$	1.391	1.391	1.392	1.390	1.392	1.390	1.389								

[a] Bond lengths are reported in Å and angles are given in degrees.

Table 2. Structure Data of the Optimized Anionic PANs[a]

geometrical parameter	p-Me	p-CF_3	p-Hex	p-Et	p-OMe	p-COMe	geometrical parameter	p-Me	p-CF_3	p-Hex	p-Et	p-OMe	p-COMe
C_1-O_1	1.278	1.276	1.278	1.278	1.278	1.273	$O_1-C_1-C_2$	118.9	118.9	118.9	118.9	118.8	119.1
C_1-C_2	1.457	1.456	1.457	1.457	1.457	1.458	$C_1-C_2-C_3$	121.9	122.0	121.9	121.9	121.9	121.9
C_2-C_3	1.389	1.387	1.388	1.388	1.388	1.388	C_1-C_2-N	108.7	108.4	108.7	108.7	108.8	108.5
C_3-C_4	1.431	1.431	1.431	1.431	1.431	1.431	C_2-N-H	105.5	105.0	105.5	105.4	105.6	105.3
C_4-O_2	1.265	1.264	1.265	1.265	1.266	1.263	$C_2-N-C_{1'}$	133.8	134.2	133.8	133.8	133.3	134.5
C_4-C_{4a}	1.470	1.470	1.470	1.470	1.470	1.472	$C_2-C_3-C_4$	121.9	122.1	122.2	122.2	122.3	122.1
$C_{4a}-C_5$	1.399	1.399	1.399	1.399	1.399	1.399	$H-N-C_{1'}$	120.3	120.4	120.4	120.4	120.5	119.9
C_5-C_6	1.387	1.387	1.387	1.387	1.387	1.387	$C_{1'}-C_{2'}-C_{3'}$	121.5	121.5	121.4	121.4	121.8	121.4
C_6-C_7	1.409	1.408	1.409	1.409	1.409	1.407	$C_{1'}-C_{6'}-C_{5'}$	120.6	120.6	120.5	120.5	121.2	120.4
C_7-C_8	1.384	1.384	1.384	1.384	1.384	1.385	$C_{8a}-C_1-C_2$	117.2	117.2	117.2	117.2	117.1	117.2
C_8-C_{8a}	1.407	1.406	1.407	1.407	1.407	1.405	$C_2-N-C_{1'}-C_{2'}$	−175.1	−177.1	175.2	175.2	−173.9	176.1
$C_{4a}-C_{8a}$	1.420	1.418	1.420	1.420	1.420	1.417	$O_1-C_1-C_2-N$	0.4	0.4	−0.5	−0.5	0.5	−0.3
C_2-N	1.374	1.377	1.375	1.374	1.373	1.375	$H-N-C_2-C_1$	2.2	2.3	−2.2	−2.1	2.0	−2.4
$N-H$	1.051	1.055	1.052	1.052	1.051	1.053	$C_1-C_2-C_3-C_4$	1.5	1.7	−1.6	−1.6	1.6	−1.6
$N-C_{1'}$	1.365	1.356	1.364	1.364	1.368	1.356	$C_2-C_3-C_4-C_{4a}$	−0.1	−0.3	0.3	0.2	−0.2	0.3
$C_{1'}-C_{2'}$	1.413	1.418	1.413	1.414	1.414	1.420	$C_2-C_1-C_{8a}-C_8$	−179.3	−179.3	179.5	179.3	−179.3	179.3
$C_{2'}-C_{3'}$	1.385	1.379	1.385	1.385	1.382	1.374	$C_{8a}-C_1-C_2-N$	−179.3	−179.3	179.1	179.3	−179.2	179.5
$C_{3'}-C_{4'}$	1.402	1.402	1.402	1.402	1.400	1.411	$C_1-C_2-N-C_{1'}$	−170.5	−170.1	170.0	170.5	−169.6	172.0
$C_{4'}-R$	1.496	1.474	1.497	1.498	1.371	1.457	$O_1-C_2-C_4-O_2$	−177.8	−177.8	177.6	177.6	−177.6	177.7
$C_{1'}-C_{6'}$	1.410	1.415	1.411	1.410	1.406	1.415	$C_2-N-C_{1'}-C_{6'}$	7.0	4.6	−6.8	−6.9	7.9	−5.4
$C_{6'}-C_{5'}$	1.390	1.384	1.390	1.390	1.395	1.383	$O_1-H(N)$	1.822	1.800	1.821	1.820	1.824	1.816
$C_{5'}-C_{4'}$	1.398	1.398	1.398	1.398	1.394	1.407							

geometrical parameter	p-Bu	p-Cl	p-COOH	p-Br	p-NO_2	PAN	geometrical parameter	p-Bu	p-Cl	p-COOH	p-Br	p-NO_2	PAN
C_1-O_1	1.278	1.277	1.274	1.277	1.268	1.278	$O_1-C_1-C_2$	118.9	118.8	119.1	118.8	119.2	118.9
C_1-C_2	1.457	1.456	1.458	1.456	1.462	1.457	$C_1-C_2-C_3$	121.9	122.0	122.0	122.0	121.8	121.9
C_2-C_3	1.388	1.387	1.388	1.387	1.387	1.388	C_1-C_2-N	108.8	108.6	108.4	108.6	108.5	108.7
C_3-C_4	1.431	1.431	1.431	1.431	1.431	1.431	C_2-N-H	105.5	105.2	105.2	105.2	105.7	105.4
C_4-O_2	1.265	1.264	1.263	1.264	1.260	1.265	$C_2-N-C_{1'}$	133.7	133.7	134.6	133.6	134.6	134.0
C_4-C_{4a}	1.470	1.470	1.471	1.470	1.474	1.470	$C_2-C_3-C_4$	122.2	122.1	122.1	122.1	122.0	122.2
$C_{4a}-C_5$	1.399	1.399	1.399	1.399	1.398	1.399	$H-N-C_{1'}$	120.3	120.6	120.0	120.6	119.5	120.2
C_5-C_6	1.388	1.387	1.387	1.387	1.388	1.387	$C_{1'}-C_{2'}-C_{3'}$	121.4	121.8	121.4	121.9	121.4	121.5
C_6-C_7	1.409	1.408	1.407	1.408	1.406	1.409	$C_{1'}-C_{6'}-C_{5'}$	120.5	120.9	120.5	121.1	120.5	120.6
C_7-C_8	1.384	1.384	1.384	1.384	1.385	1.384	$C_{8a}-C_1-C_2$	117.2	117.2	117.2	117.1	117.3	117.2
C_8-C_{8a}	1.407	1.407	1.405	1.407	1.404	1.407	$C_2-N-C_{1'}-C_{2'}$	175.1	175.8	176.4	175.8	−175.3	−175.6
$C_{4a}-C_{8a}$	1.420	1.419	1.417	1.419	1.414	1.420	$O_1-C_1-C_2-N$	−0.4	−0.5	−0.2	−0.4	0.0	0.3
C_2-N	1.375	1.376	1.376	1.376	1.371	1.375	$H-N-C_2-C_1$	−2.4	−2.2	−2.5	−2.3	2.5	2.3
$N-H$	1.051	1.053	1.054	1.053	1.052	1.051	$C_1-C_2-C_3-C_4$	−1.6	−1.7	−1.6	−1.8	1.5	1.7
$N-C_{1'}$	1.364	1.361	1.355	1.360	1.358	1.364	$C_2-C_3-C_4-C_{4a}$	0.2	0.3	0.2	0.3	−0.1	−0.2
$C_{1'}-C_{2'}$	1.413	1.414	1.420	1.415	1.419	1.414	$C_2-C_1-C_{8a}-C_8$	179.2	179.3	179.3	179.3	−179.3	−179.3
$C_{2'}-C_{3'}$	1.385	1.385	1.375	1.385	1.376	1.386	$C_{8a}-C_1-C_2-N$	179.4	179.3	179.4	179.3	−179.6	−179.4
$C_{3'}-C_{4'}$	1.402	1.395	1.408	1.394	1.403	1.399	$C_1-C_2-N-C_{1'}$	170.0	169.2	171.7	169.1	−172.9	−169.9
$C_{4'}-R$	1.497	1.748	1.447	1.902	1.419	1.098	$O_1-C_2-C_4-O_2$	177.6	177.5	177.8	177.5	−177.7	−177.7
$C_{1'}-C_{6'}$	1.411	1.412	1.416	1.412	1.416	1.411	$C_2-N-C_{1'}-C_{6'}$	−7.2	−5.9	−5.1	−6.0	6.3	5.9
$C_{6'}-C_{5'}$	1.390	1.390	1.382	1.390	1.381	1.390	$O_1-H(N)$	1.823	1.810	1.809	1.810	1.824	1.821
$C_{5'}-C_{4'}$	1.398	1.391	1.405	1.390	1.400	1.395							

geometrical parameter	m-Me	m-Et	m-Cl	m-COOH	m−F	m-NO_2	m-CN	geometrical parameter	m-Me	m-Et	m-Cl	m-COOH	m−F	m-NO_2	m-CN
C_1-O_1	1.278	1.277	1.277	1.275	1.277	1.265	1.276	$O_1-C_1-C_2$	118.9	118.9	118.9	118.9	118.9	118.9	118.8
C_1-C_2	1.457	1.457	1.456	1.458	1.456	1.466	1.456	$C_1-C_2-C_3$	121.9	121.9	122.0	121.9	121.9	121.5	122.1
C_2-C_3	1.388	1.388	1.387	1.387	1.387	1.384	1.387	C_1-C_2-N	108.7	108.7	108.6	108.7	108.6	109.2	108.5
C_3-C_4	1.431	1.431	1.431	1.431	1.431	1.432	1.431	C_2-N-H	105.4	105.5	105.2	105.6	105.2	107.1	105.2
C_4-O_2	1.265	1.265	1.264	1.264	1.265	1.259	1.264	$C_2-N-C_{1'}$	134.0	133.9	133.6	133.4	133.8	132.7	133.3
C_4-C_{4a}	1.470	1.470	1.470	1.471	1.470	1.474	1.471	$C_2-C_3-C_4$	122.3	122.2	122.1	122.2	122.2	122.2	122.1
$C_{4a}-C_5$	1.399	1.399	1.399	1.399	1.399	1.397	1.399	$H-N-C_{1'}$	120.2	120.2	120.6	120.4	120.5	119.8	120.7
C_5-C_6	1.387	1.387	1.387	1.387	1.387	1.388	1.387	$C_{1'}-C_{2'}-C_{3'}$	122.4	122.4	120.4	121.3	120.0	120.3	121.1
C_6-C_7	1.408	1.409	1.408	1.408	1.408	1.406	1.408	$C_{1'}-C_{6'}-C_{5'}$	120.0	120.1	120.4	120.8	120.6	120.4	121.0
C_7-C_8	1.384	1.384	1.384	1.384	1.384	1.385	1.384	$C_{8a}-C_1-C_2$	117.2	117.1	117.1	117.2	117.2	117.5	117.2
C_8-C_{8a}	1.407	1.407	1.406	1.406	1.407	1.404	1.406	$C_2-N-C_{1'}-C_{2'}$	175.6	175.3	175.8	175.4	175.5	171.9	176.2
$C_{4a}-C_{8a}$	1.420	1.420	1.419	1.418	1.419	1.414	1.418	$O_1-C_1-C_2-N$	−0.3	−0.3	−0.3	−0.3	−0.3	−0.1	−0.4
C_2-N	1.375	1.375	1.377	1.375	1.377	1.368	1.377	$H-N-C_2-C_1$	−2.3	−2.4	−2.5	−2.6	−2.5	−3.1	−2.7
$N-H$	1.051	1.051	1.053	1.051	1.052	1.046	1.053	$C_1-C_2-C_3-C_4$	−1.6	−1.7	−1.8	−2.0	−1.7	−2.3	−2.0
$N-C_{1'}$	1.364	1.364	1.360	1.363	1.361	1.371	1.359	$C_2-C_3-C_4-C_{4a}$	0.2	0.1	0.2	0.3	0.3	0.4	0.4
$C_{1'}-C_{2'}$	1.413	1.414	1.415	1.408	1.414	1.404	1.410	$C_2-C_1-C_{8a}-C_8$	179.3	179.2	179.2	179.2	179.3	179.0	179.2
$C_{2'}-C_{3'}$	1.388	1.388	1.382	1.392	1.379	1.388	1.395	$C_{8a}-C_1-C_2-N$	179.5	179.5	179.4	179.3	179.4	179.6	179.3
$C_{3'}-C_{4'}$	1.403	1.403	1.394	1.404	1.391	1.401	1.409	$C_1-C_2-N-C_{1'}$	170.0	170.1	168.7	168.1	169.5	169.1	167.2
$C_{3'}-R$	1.499	1.501	1.750	1.465	1.354	1.439	1.424	$O_1-C_2-C_4-O_2$	177.6	177.7	177.6	177.5	177.6	177.0	177.5
$C_{1'}-C_{6'}$	1.410	1.410	1.412	1.414	1.413	1.413	1.415	$C_2-N-C_{1'}-C_{6'}$	−5.7	−6.5	−5.7	−6.3	−6.0	−10.1	−5.5
$C_{6'}-C_{5'}$	1.390	1.391	1.388	1.392	1.389	1.393	1.389	$O_1-H(N)$	1.821	1.823	1.811	1.824	1.813	1.868	1.808
$C_{5'}-C_{4'}$	1.394	1.393	1.396	1.390	1.396	1.389	1.391								

[a] Bond lengths are reported in Å and angles are given in degrees.

Table 3. Structure Data of the Optimized PAN Dianions[a]

geometrical parameter	PAN	p-Cl	m-Cl	p-Me	m-Me
C_1-O_1	1.312	1.310	1.310	1.311	1.311
C_1-C_2	1.435	1.435	1.435	1.435	1.436
C_2-C_3	1.411	1.411	1.411	1.411	1.411
C_3-C_4	1.420	1.422	1.421	1.422	1.422
C_4-O_2	1.287	1.286	1.286	1.287	1.287
C_4-C_{4a}	1.464	1.465	1.465	1.464	1.464
$C_{4a}-C_5$	1.403	1.403	1.403	1.403	1.403
C_5-C_6	1.389	1.389	1.389	1.389	1.389
C_6-C_7	1.419	1.418	1.418	1.419	1.419
C_7-C_8	1.383	1.383	1.383	1.383	1.383
C_8-C_{8a}	1.415	1.415	1.414	1.415	1.415
$C_{4a}-C_{8a}$	1.444	1.442	1.441	1.444	1.443
C_2-N	1.389	1.388	1.388	1.388	1.388
$N-H$	1.078	1.080	1.081	1.077	1.077
$N-C_{1'}$	1.345	1.344	1.342	1.346	1.345
$C_{1'}-C_{2'}$	1.429	1.430	1.433	1.428	1.429
$C_{2'}-C_{3'}$	1.384	1.383	1.377	1.384	1.385
$C_{3'}-C_{4'}$	1.407	1.400	1.399	1.408	1.410
$C_{4'}-R$	1.765	1.496			
$C_{3'}-R$			1.772		1.501
$C_{1'}-C_{6'}$	1.426	1.427	1.427	1.425	1.425
$C_{6'}-C_{5'}$	1.387	1.387	1.384	1.388	1.387
$C_{5'}-C_{4'}$	1.405	1.399	1.408	1.406	1.404
$O_1-C_1-C_2$	119.2	119.2	119.2	119.2	119.2
$C_1-C_2-C_3$	123.5	123.5	123.5	123.5	123.4
C_1-C_2-N	107.1	107.0	106.9	107.1	107.1
C_2-N-H	101.3	101.2	101.1	101.4	101.3
$C_2-N-C_{1'}$	135.9	135.8	135.8	135.8	136.2
C_2-C_3-C_4	122.8	122.6	122.7	122.7	122.8
$H-N-C_{1'}$	122.4	122.6	122.8	122.3	122.2
$C_{1'}-C_{2'}$-$C_{3'}$	122.1	122.3	120.5	122.0	122.9
$C_{1'}-C_{6'}-C_{5'}$	121.2	121.5	121.1	121.1	120.7
$C_{8a}-C_1-C_2$	115.5	115.6	115.6	115.5	115.6
$C_2-N-C_{1'}-C_{2'}$	−179.3	179.2	178.7	−179.8	178.8
$O_1-C_1-C_2-N$	0.9	−0.9	−0.7	0.9	−0.6
$H-N-C_2-C_1$	1.3	−1.1	−1.2	1.1	−0.9
$C_1-C_2-C_3$-C_4	1.0	−1.0	−0.9	1.1	−0.8
C_2-C_3-C_4-C_{4a}	−0.3	0.2	0.2	−0.2	0.2
$C_2-C_1-C_{8a}-C_8$	−179.9	179.9	179.9	−179.9	180.0
$C_{8a}-C_1-C_2-N$	−178.7	178.7	178.9	−178.7	178.9
$C_1-C_2-N-C_{1'}$	−171.2	171.4	172.3	−170.7	173.6
$O_1-C_2-C_4-O_2$	−178.4	178.5	178.6	−178.5	178.8
$C_2-N-C_{1'}-C_{6'}$	1.5	−1.6	−2.0	1.4	−1.5
$O_1-H(N)$	1.686	1.678	1.673	1.689	1.689

[a] Bond lengths are reported in Å and angles are given in degrees.

$C_2-N-C_{1'}-C_{6'}$ dihedral angle. Only the global minima are reported in Table 1. Positive signs of the $C_2-N-C_{1'}-C_{6'}$ dihedral angle indicate that the carbon atoms $C_{2'}$ and $C_{3'}$ are located behind the paper plane in Figure 1. In all compounds the energy differences between the minima with positive and negative $C_2-N-C_{1'}-C_{6'}$ dihedral angles are small. For the PAN system we scanned the PES along the $C_2-N-C_{1'}-C_{6'}$ dihedral angle. The rotation barrier is below 0.5 kcal/mol which explains the floppy behavior of this coordinate in structure optimizations.

The m-F PAN shows the largest deviation from planarity (20.1 degrees), while the p-NO_2 PAN shows the smallest (14.8 degrees). The absolute value of the dihedral angle increases with the electron donor capacity of the *para* substituent along the series p-NO_2 < p-CF_3 < p-Br < H < p-Et < p-Me < p-MeO. This behavior can be straightforwardly explained by the resonance structures depicted in Figure 2 and discussed later on.

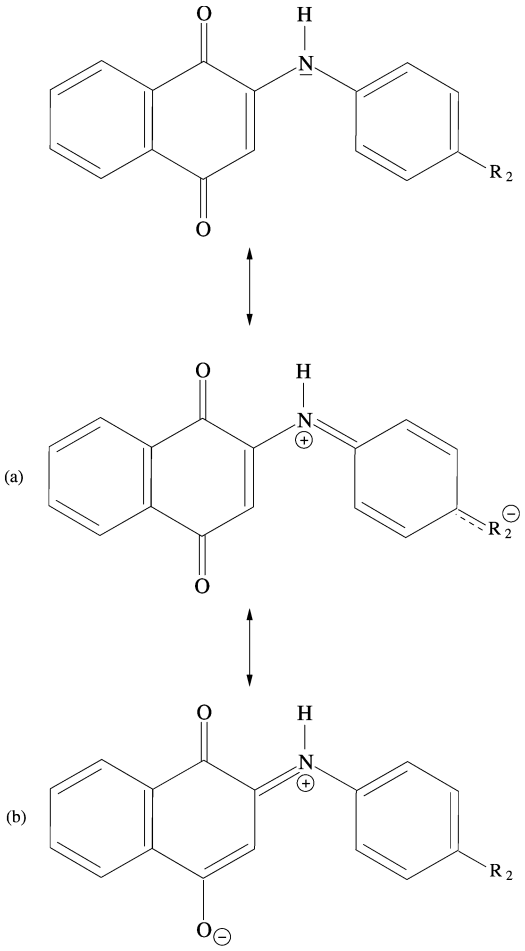

Figure 2. Resonance structures for *para*-substituted phenyl substituents. In (a) R_2 is the dominating electron acceptor, whereas in (b) the quinone oxygen O_2 dominates.

When an electron is added to the neutral PANs and the corresponding radical anion is formed, the $C_2-N-C_{1'}-C_{6'}$ dihedral angles decrease by 10 degrees or more as Table 2 shows. The m-NO_2 anion possesses the largest $C_2-N-C_{1'}-C_{6'}$ dihedral angle (10.1 degrees), while the p-CF_3 anion has the smallest dihedral angle (4.6 degrees). If a second electron is added to form the corresponding dianion, then the PANs become practical planar with $C_2-N-C_{1'}-C_{6'}$ dihedral angles of around 1 degree or less. As examples the optimized structure parameters of the H, p-Cl, m-Cl, p-Me, and m-Me PAN dianions are listed in Table 3.

Another structural detail was observed in the naphthoquinone moiety. At first glance one might expect that this moiety is perfectly planar. However, we found a small rumpling in the neutral and anionic systems in the $C_1-C_2-C_3-C_4$ dihedral angles (see Tables 1 and 2). Because these values are in the range of 2 degrees and, thus, closed to the numerical accuracy of deMon2k we first attributed them to noise in the numerical integration of the exchange-correlation potential. However, the rumpling remained even when

Table 4. Frequencies [cm^{-1}] of Selected Neutral PANs

molecule	frequencies (cm^{-1})									
PAN	14.7	48.5	80.8	91.6	121.7	150.7	196.7	211.6	237.6	259.9
	293.2	381.1	392.5	405.6	430.4	452.7	457.1	476.5	507.6	550.7
	578.7	604.0	654.2	658.7	688.1	708.3	711.4	712.4	728.7	757.5
	770.7	797.8	799.5	814.7	842.9	862.0	877.3	891.9	933.1	953.8
	963.6	985.3	1006.7	1019.4	1034.1	1037.9	1085.2	1090.7	1121.4	1135.0
	1136.4	1162.5	1205.1	1228.6	1247.3	1276.8	1313.4	1337.9	1363.4	1414.8
	1430.7	1457.4	1470.5	1490.9	1496.9	1546.2	1616.3	1626.3	1640.5	1648.5
	1658.5	1679.3	1710.7	3094.3	3102.4	3105.6	3109.1	3110.1	3117.4	3121.2
	3122.6	3143.4	3153.4	3288.3						
p-CF_3	13.0	29.1	32.0	56.0	67.0	108.2	121.8	145.3	162.8	170.3
	205.3	226.0	254.6	290.7	355.4	381.2	383.2	389.6	402.3	405.1
	436.6	452.9	471.2	479.1	498.1	556.8	566.6	574.5	605.2	620.7
	656.5	663.6	708.5	711.2	715.0	728.4	754.7	760.8	767.0	789.5
	797.3	800.0	816.7	837.5	863.6	891.1	937.5	946.0	960.9	983.2
	1006.1	1013.7	1037.2	1073.6	1087.9	1104.7	1113.2	1135.4	1139.9	1161.5
	1182.6	1207.0	1223.2	1244.5	1278.5	1297.2	1323.5	1336.6	1367.7	1409.5
	1431.3	1450.5	1470.8	1491.8	1508.3	1567.9	1616.8	1624.2	1639.2	1654.5
	1670.7	1684.1	1712.1	3109.0	3111.6	3117.2	3123.8	3124.9	3130.2	3133.9
	3153.2	3171.5	3277.4							
m−F	23.5	34.5	81.5	83.9	123.4	152.6	197.0	200.2	211.0	240.3
	258.2	279.9	381.8	392.8	409.2	431.3	442.7	452.6	464.1	489.2
	512.4	551.7	577.2	596.1	655.6	656.8	664.0	708.7	712.9	716.5
	720.3	759.2	763.1	767.5	792.8	797.8	823.8	835.8	849.9	890.5
	909.7	949.9	959.9	981.8	1007.1	1018.6	1036.9	1069.6	1088.8	1111.8
	1132.4	1143.8	1154.3	1205.8	1237.4	1266.3	1273.8	1309.3	1342.4	1363.8
	1417.1	1431.4	1447.9	1472.5	1490.4	1511.8	1552.3	1618.2	1632.5	1639.6
	1653.7	1665.5	1680.8	1712.5	3107.6	3113.6	3116.2	3125.2	3130.6	3133.0
	3149.4	3156.5	3169.1	3294.6						

improving the grid accuracy. A closer look at the experimental available crystallographic data[37,38] revealed that this rumpling is in fact in agreement with experiments. Similar deviations from planarity are found in crystallographic data of other aromatic compounds, too.[39] The aromaticity is usually not substantially effected by these deviations from planarity.[40]

Because the nitrogen atom modulates the charge transfer between the quinone and the *para*- or *meta*-substituted phenyl ring it is interesting to analyze the bonding in the quinone ring with respect to the phenyl substituent. Along the series p-NO_2 < p-CF_3 < p-Br < H < p-Et < p-Me < p-OMe the electron-donor capacity of the phenyl substituent increases. As a result we observe elongation of the N−$C_{1'}$ bond (from 1.376 Å to 1.387 Å), contraction of the C_2−N bond (from 1.356 Å to 1.349 Å), elongation of the C_2−C_3 bond (from 1.368 Å to 1.375 Å), contraction of the C_3-C_4 bond (from 1.446 Å to 1.437 Å), and elongation of the C_4−O_2 bond (from 1.239 Å to 1.243 Å) in the neutral PANs. These bond length changes can be explained by the two possible resonance structures for the *para*-substituted PANs depicted in Figure 2. If the R_2 electron acceptor strength is larger than that of the quinone oxygen, O_2, then the weight of resonance structure (a) in Figure 2 increases. As a result the N−$C_{1'}$ bond is contracted due to its double bond character in the (a) resonance structure. On the other hand, if the quinone oxygen O_2 is the dominant electron acceptor in the system, then the weight of resonance structure (b) in Figure 2 will be increased. In this situation the C_2−N bond is shortened due to its double bond character in resonance structure (b).

The other bond length changes are direct consequences of the preference of one or the other resonance structure in Figure 2. Besides these changes in the covalent bonds a slight elongation of the O_1···H(N) distance is also noticed (Table 1). In the corresponding *meta*-substituted compounds a similar trend can be found in the series m-NO_2 > m-CN > mF > m-Cl > m-Et > m-Me. However, the distortions are smaller as in the *para*-substituted systems because no equivalent resonance structures can be formulated. In the anionic systems the same general trend can be observed (see Table 2). The only exception is in the C_3−C_4 bond which is around 1.43 Å long independently from the substitution. In all cases, going from the neutral to the radical anion to the dianion (PAN → PAN $^{\bullet-}$ → PAN^{2-}) a gradual contraction of the O_1···H(N) distance occurs. This is due to the increased density at the quinone oxygen O_1 that strengthen the hydrogen bridge.

III-B. Vibrational Analysis. In order to characterize the optimized structures and to simulate the infrared (IR) spectra a harmonic frequency analysis was performed for selected molecules using the VWN optimized structures. The results for the neutral and anionic H, p-CF_3, and m-F PAN are listed in Tables 4 and 5, respectively. Similar results were obtained for other structures.

As can be seen from Tables 4 and 5 all calculated frequencies are positive, and, therefore, the optimized structures are minima on the PES. A closer inspection of

Table 5. Frequencies [cm^{-1}] of Selected Anionic PANs

molecule	frequencies (cm^{-1})									
PAN	24.7	40.7	84.4	101.2	137.1	166.5	199.1	228.6	245.4	255.2
	286.5	371.3	387.1	407.4	430.3	459.6	470.4	481.4	497.5	551.5
	577.1	606.9	641.0	654.7	672.8	685.3	707.3	714.8	719.4	735.2
	765.2	773.7	798.2	817.9	822.6	836.1	848.7	866.8	908.0	919.7
	934.8	948.4	1003.1	1016.5	1025.6	1034.4	1074.3	1080.5	1104.2	1122.1
	1128.4	1158.0	1190.0	1215.8	1230.7	1279.0	1290.8	1310.7	1381.5	1404.7
	1417.8	1453.5	1460.6	1475.0	1491.3	1550.7	1554.2	1569.5	1584.4	1600.7
	1634.0	1646.3	1664.6	3077.1	3087.2	3089.2	3090.8	3099.6	3104.0	3111.8
	3115.4	3133.2	3139.7	3159.1						
p-CF_3	11.2	20.8	30.7	59.8	72.9	114.4	135.8	142.4	169.0	173.1
	206.6	224.2	252.0	287.9	364.1	373.1	382.9	391.6	398.0	414.4
	431.7	459.5	471.6	482.8	495.1	560.6	565.3	568.1	594.0	619.1
	640.3	662.7	686.8	708.0	717.0	717.8	739.3	745.8	762.8	770.1
	776.1	799.3	834.3	848.3	855.9	883.9	917.3	929.6	938.6	954.4
	1007.1	1020.0	1026.6	1050.8	1078.0	1089.4	1095.3	1107.7	1130.1	1147.7
	1154.9	1191.8	1211.7	1230.1	1278.6	1288.3	1301.1	1353.1	1392.0	1395.9
	1420.6	1456.0	1467.6	1481.7	1501.4	1555.0	1562.4	1571.9	1594.6	1598.1
	1639.4	1646.2	1668.5	3081.7	3091.8	3095.0	3102.4	3106.3	3113.8	3116.8
	3123.4	3143.7	3174.1							
m−F	24.2	33.6	76.8	96.6	141.8	165.6	198.2	207.3	220.9	237.0
	260.6	277.2	371.3	394.0	406.8	434.0	442.6	458.7	472.4	497.3
	510.5	550.5	581.3	589.3	642.8	652.5	662.3	686.7	690.8	708.9
	716.7	740.4	753.2	766.1	768.6	793.8	805.5	836.0	850.6	866.1
	894.3	934.9	936.5	949.5	995.6	1015.4	1023.9	1058.7	1078.1	1102.3
	1115.3	1136.8	1148.8	1191.8	1230.0	1243.8	1263.8	1288.9	1313.6	1375.2
	1406.6	1418.2	1446.7	1461.0	1482.9	1500.5	1553.4	1556.1	1571.3	1589.0
	1605.7	1637.5	1645.9	1669.5	3078.9	3090.6	3095.9	3100.6	3107.8	3117.7
	3122.9	3134.0	3143.1	3168.6						

these tables reveals that the low frequencies of these systems are small. The first two vibrational modes of the neutral PAN (14.7 and 48.5 cm^{-1}) are rotations around the $C_1-C_2-N-C_{1'}$ and $C_2-N-C_{1'}-C_{6'}$ dihedral angles. The following two frequencies (80.8 and 91.6 cm^{-1}) are deformation modes in the naphthoquinone moiety that couple with the above-described two dihedral angles. In the substituted PANs the situation is very similar. A main difference is the coupling of the internal rotations of substituent groups, like the CF_3, to the low lying frequencies of the $C_1-C_2-N-C_{1'}$ and $C_2-N-C_{1'}-C_{6'}$ dihedral angles. In the corresponding anionic systems this coupling is usually reduced.

In Figure 3 the simulated infrared spectrum (IR) of the PAN molecule is depicted. For the simulation the harmonic frequencies were broadened by 5 cm^{-1}. Five significant groups of signals can be distinguished. The finger print bands (modes 58 and 59 in Table 4; labeled with **A** in Figure 3) appear at around 1350 cm^{-1}. At 1546 cm^{-1} (mode 66 in Table 4; labeled with **B** in Figure 3) the in-plane N−H···O deformation band appears. The C═C valence bands (modes 67, 69, 70, and 71 in Table 4; labeled with **C** in Figure 3) dominate the IR spectrum of the PAN. The two shoulders at higher wave numbers (modes 72 and 73 in Table 4; labeled **D** in Figure 3) correspond to the two C═O valence bands (C═O_2 at 1680 cm^{-1} and C═O_1 at 1710 cm^{-1}). The N−H stretch band (mode 84 in Table 4; labeled **E** in Figure 3) appears in our simulation at 3288 cm^{-1}. This is in fair agreement with the experimental observation[41] where a sharp band at 3310 cm^{-1} was assigned to the N−H stretch vibration.

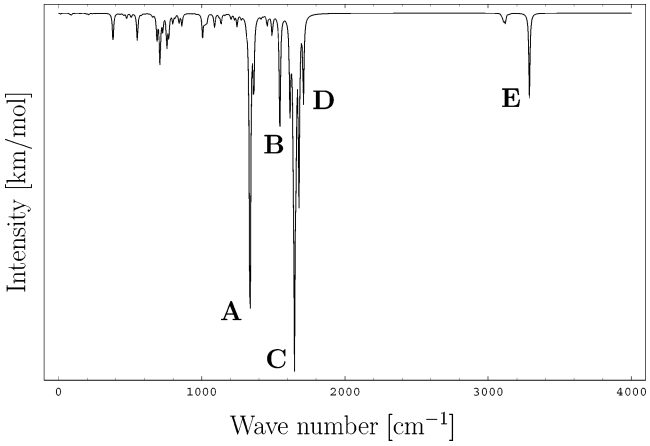

Figure 3. Simulated IR spectrum for the PAN molecule. A broadening of 5 cm^{-1} was applied. See the text for the discussion of the marked bands.

III-C. Electronic Structure Analysis. At first glance the nonplanarity of the neutral PAN derivatives might be assigned to steric interactions. However, this is contradictory to our finding that anionic systems are more planar and that the dianions are almost perfectly planar. Therefore, the electronic structure should be mainly responsible for these structural changes. For this reason we investigated the π orbital occupation of the unsubstituted PAN. In order to

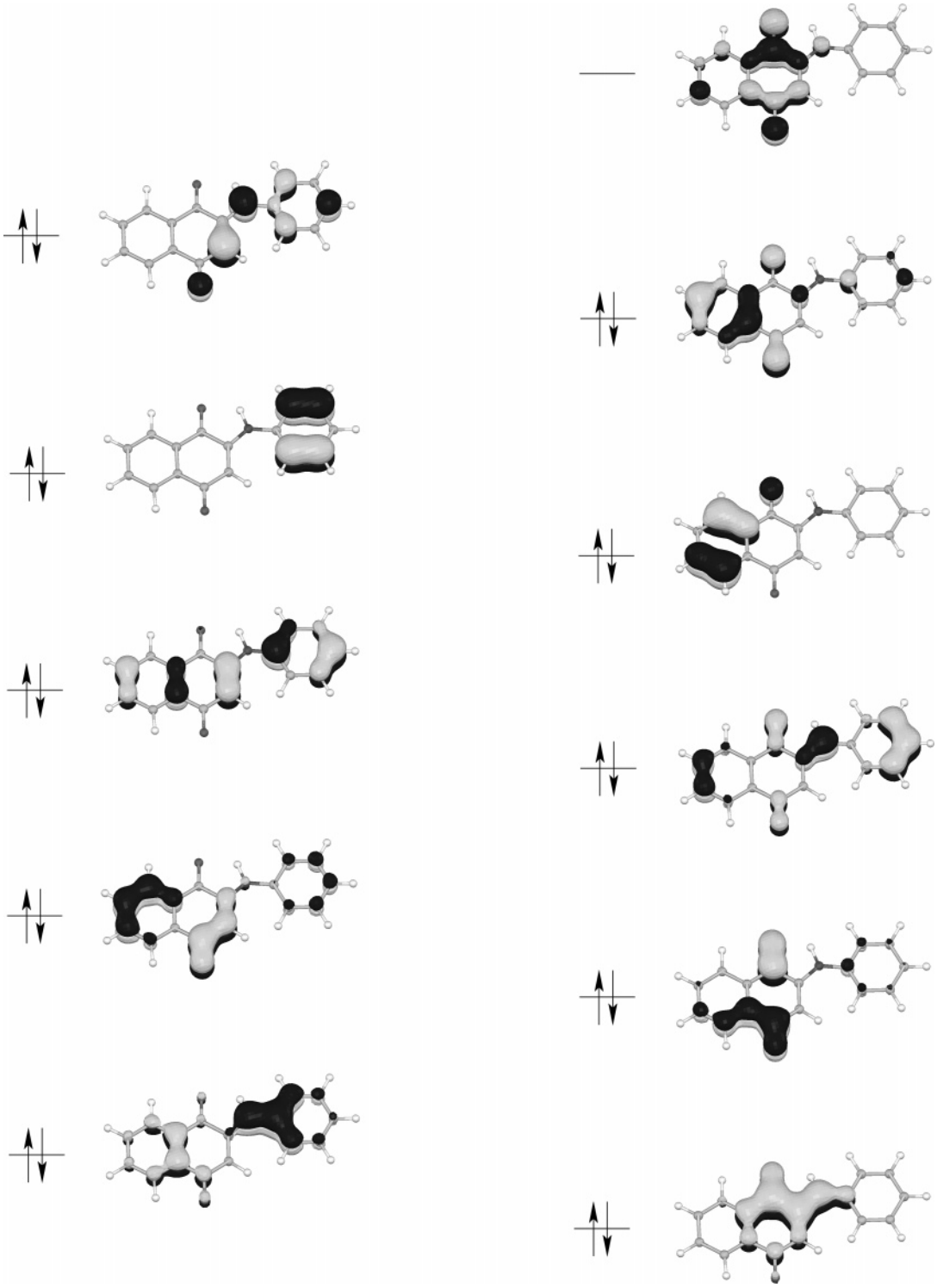

Figure 4. The occupied π orbitals of the PAN molecule in ascending ordering. The LUMO is depicted, too.

simplify the analysis we enforced planarity of the PAN molecule in these calculations. The occupied π orbitals and the lowest unoccupied molecular orbital (LUMO) are graphically displayed in Figure 4. This figure shows that the PAN molecule has ten double occupied π orbitals. The highest occupied π orbital represents the second highest occupied molecular orbital. The LUMO is a π orbital, too. In the PAN systems the planar structure distorts and breaks the conjugation over the whole system. Subsystems with 6 and 14 π electrons are generated, each of them aromatic by itself according to Hückel's rule. The formation of these subsystems manifests itself in the C_2-N and $N-C_{1'}$ bond lengths. In the neutral PAN systems the C_2-N bond is always shorter than the $N-C_{1'}$ bond. As a consequence resonance structure (b) in Figure 2 is dominant in all neutral PAN systems. Formal counting of the electron pairs in this resonance structure reveals immediately the 6 and 14 π electron subsystems. Such forming of aromatic subsystems has been observed in polycyclic hydrocarbons, too.[42] If the PAN compound is reduced to form the corresponding

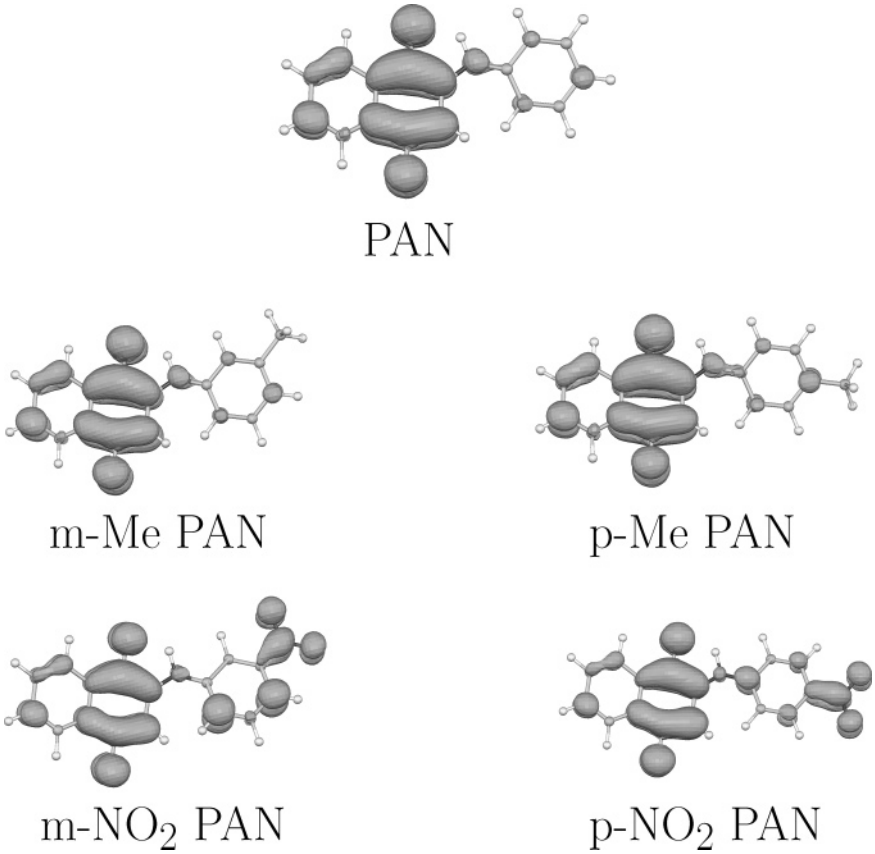

Figure 5. Spin density plots for selected PAN anions.

dianionic system, then the two additional electrons occupy the LUMO π orbital. As can be seen from Figure 4 the LUMO is mainly located in the naphthoquinone moiety. Therefore, the two extra electrons are added to this subsystem. In order to keep it aromatic an electron pair must be expelled. The electron pair flip from the C_2-N to the $N-C_{1'}$ bond by going from resonance structure (b) to (a) in Figure 2 will, therefore, stabilize anionic systems. In fact, in all dianionic PAN systems the $N-C_{1'}$ bond is shorter than the C_2-N bond. The increased double bond character of the $N-C_{1'}$ bond then forces the molecule to planarity.

In Figure 5 spin density plots for H, m-Me, p-Me, m-NO_2, and p-NO_2 PAN anions are depicted. As these plots show the anionic radical electron is mainly localized in the π system of the quinone fragment. The spin density distribution in this moiety is very similar for all five anions independently from the substitution pattern. In m-NO_2 and p-NO_2 PAN anions a substantial part of the spin density is located at the nitro group. An interesting detail represents the spin density distribution in the phenyl group. Usually, spin densities are found in ortho and para positions of this group. However, in the m-NO_2 and p-NO_2 PAN anions this pattern is modified. Therefore, we can conclude that strong electron acceptor substituents modify the spin density distribution in the phenyl ring but not in the naphthoquinone moiety.

III-D. Correlation of Electron Affinities with Half-Wave Potentials. The vertical and adiabatic electron affinities (VEAs and AEAs) were calculated with the local and gradient corrected functionals described in the Computational section. The obtained results for VEAs and AEAs are listed in Table 6 together with the experimental half-wave potentials. In Table 6 the molecules are ordered according to their decreasing electron affinities. No qualitative difference between the VWN and GGA trend is observed. Table 6 shows that the electrochemical results obtained for p-COOH PAN (−917 mV) and m-COOH PAN (−880 mV) are very

Table 6. Calculated Vertical and Adiabatic Electron Affinities [eV] with the VWN and BLYP Functional[a]

	VWN		BLYP		
molecule	vertical	adiabatic	vertical	adiabatic	HWP
p-NO_2 PAN	2.59	2.73	2.13	2.34	−1067
m-NO_2 PAN	2.45	2.56	1.99	2.21	−1104
p-COMe PAN	2.27	2.43	1.81	2.03	−1126
m-CN PAN	2.25	2.41	1.79	2.00	−1133
p-COOH PAN	2.23	2.41	1.78	2.01	−917
p-CF_3 PAN	2.19	2.38	1.72	1.99	−1147
m-COOH PAN	2.07	2.25	1.61	1.85	−880
p-Br PAN	2.06	2.23	1.61	1.83	−1176
m-Cl PAN	2.05	2.23	1.59	1.83	−1145
p-Cl PAN	2.03	2.21	1.58	1.81	−1173
m−F PAN	2.01	2.19	1.56	1.80	−1163
H-PAN	1.90	2.07	1.45	1.67	−1209
m-Et PAN	1.87	2.04	1.42	1.64	−1216
m-Me PAN	1.87	2.04	1.42	1.64	−1213
p-Hex PAN	1.86	2.03	1.41	1.63	−1215
p-Bu PAN	1.86	2.03	1.41	1.64	−1217
p-Et PAN	1.86	2.03	1.41	1.63	−1218
p-Me PAN	1.85	2.02	1.40	1.62	−1216
p-OMe PAN	1.80	1.97	1.35	1.57	−1236

[a] The experimental values of the half-wave potential [mV] are reported, too.

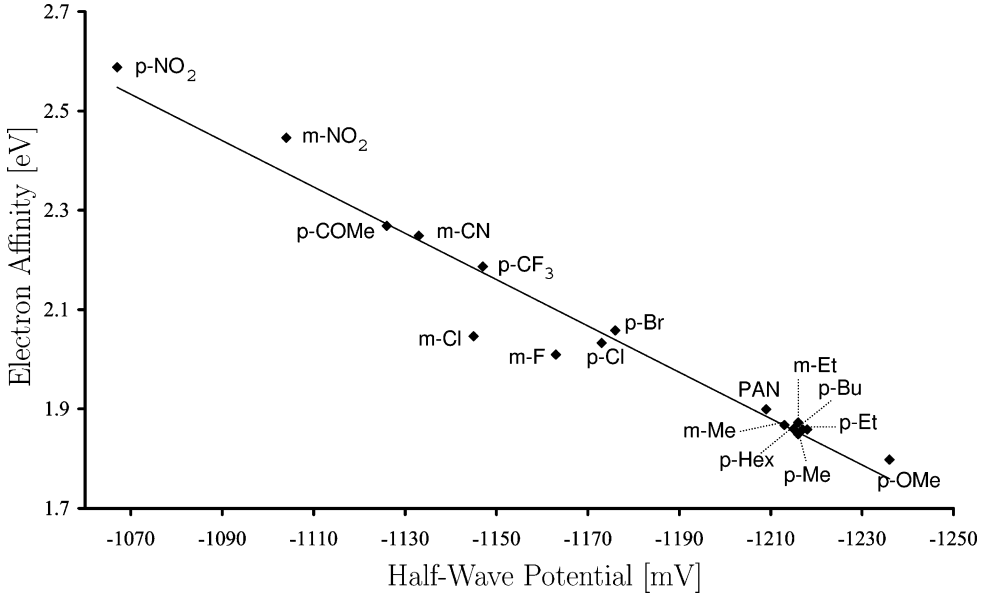

Figure 6. Correlation between the calculated (vertical VWN) electron affinities and the experimental half-wave potentials of the studied PAN systems.

different from those of the other PANs. However, the calculated electron affinities for these two compounds fit very well into the observed trends. Thus, we conclude that for these two compounds side reactions like autoprotonation or dimerization may have occurred under the experimental conditions.[43] This is in accordance with the more complex cyclic voltammograms observed for these two compounds. In order to gain more insight into the redox behavior of the PANs, the experimental HWPs for the first one-electron transfer (potential range −880 to −1236 mV), corresponding to the formation of the radical anions, were correlated with the calculated (gas-phase) electron affinities.

For obvious reasons the p-COOH and m-COOH PANs were excluded from this correlation. A linear correlation between the VEAs and the HWPs is obtained, independently from the theoretical level of calculation. Similar linear correlations between gas-phase electron affinities and half-wave potentials measured in acetonitrile have been found for other quinones, too.[44]

The correlation coefficient is around 0.98 which indicates that the one-electron transfers in the cyclic voltammogramm can be described by the Nernst equation and that the free energy of the reaction

$$\mathrm{PAN(sol)} + \mathrm{e^-(sol)} \rightleftharpoons \mathrm{PAN^{\bullet -}\ (sol)}$$

is proportional to the half-wave potential $E_{1/2}$.[45] Under this condition the following relationship between the gas-phase electron affinity $\mathrm{EA_{(g)}}$ and the half-wave potential $E_{1/2}$

$$\mathrm{EA_{(g)}} = kE_{1/2} + C$$

holds if the solvation energy differences between the neutral and anionic PAN systems is similar for all compounds and temperature effects are negligible. This explains the observation in the literature[23] that the solvent has no effect on the first redox potential of some quinone systems. In Figure 6 the VEAs, calculated at the local level, are plotted against the experimental HWPs. The COOH substituted systems are omitted. We notice a group of 6 PAN compounds with alkyl substituents very close together with low VEAs and high HWPs. An even lower VEA has the p-OMe substituted PAN. As expected, the highest electron affinities are found for strong electron acceptors like p-NO_2. All together the observed trend can be qualitatively explained by the electronic properties of the substituents.

IV. Conclusions

Density functional theory calculations have been performed for the 2-[(R-phenyl)amine]-1,4-naphthalenedione (PAN) molecule and 18 of its derivatives. Neutral, anionic, and selected dianonic PAN systems were studied with local and gradient corrected functionals. The theoretical results show that all neutral compounds are nonplanar. The nonplanarity of the neutral systems is triggered by the electronic structure of the compounds. As an example the electronic structure of the neutral PAN molecule was analyzed in detail. This system possesses 20 π electrons. The distortion from planarity breaks the conjugation and forms two aromatic subsystems with 6 and 14 π electrons. This result in a stabilization of the full system. The same effect was observed for all studied PAN derivatives.

On the other hand, the PAN dianion with 22 π electron cannot be broken down into two aromatic subsystems. As a consequence the dianions are planar and fully conjugated. This structural difference between the neutral and dianionic PAN molecule also shows that steric effects are not the driving force for the distortion from planarity.

From the theoretical study of the neutral and anionic PAN molecules a very good linear correlation between the calculated electron affinity and the experimental half-wave potential was found. An exception represent the two carbo-acid substituted compounds (m-COOH PAN and p-COOH PAN). Our investigation suggests that the measured half-wave potentials of these two compounds are strongly influenced by side reactions. It was shown that solvation energy differences and

temperature effects are negligible for the studied compounds. Therefore, the linear relationship between the electron affinities and the half-wave potentials directly reflects the reversibility of the electron transfer in these systems.

Acknowledgment. This work was financially supported by the CONACYT projects 36037-E, 40379-F, and U48775. Z.G.S. gratefully acknowledge a CONACYT Ph.D. fellowship (93252) and financial support from the Universidad de Colima.

References

(1) Bentley, R.; Campbell, I. M. *Biological Reactions of Quinones, in The Chemistry of the Quinonoid Compounds*; Patai, S., Ed.; John Wiley and Sons: New York, 1974; Chapter 13, pp 683−736.

(2) Monks, T. J.; Hanzlik, R. P.; Cohen, G. M.; Ross, D.; Graham, D. G. *Toxicol. Appl. Pharmacol.* **1992**, *112*, 2.

(3) Bishop, N. I. *The Possible Role of Plastoquinone (Q-254) in the Electron Transport System of Photosynthesis, in Quinones in Electron Transport*; Wolstenholme, G. E. W., O'Connor, C. M., Eds.; Churchill: London, 1961; pp 385−404.

(4) Brunmark, A.; Cadenas, E. *Free Radical Biol. Med.* **1988**, *7*, 435.

(5) Zuman, P. *Subtituents Effects in Organic Polarography*; Plenum Press: New York, 1967.

(6) Trebst, A. Plastoquinone in photosynthetic electron flow in chloroplasts. In *Coenzyme Q*; Wiley: 1985.

(7) Huntington, J. L.; Davis, D. G. *J. Electron. Soc.* **1971**, *118*, 57.

(8) Li, C. Y.; Caspar, M. L.; Dixon, D. W. *Electrochim. Acta* **1980**, *25*, 1135. Qureshi, G. A.; Ireland, N. *Bull. Soc. Chim. Belg.* **1981**, *90*, 223.

(9) Stradins, J.; Glezer, V.; Turovska, B.; Markava, E.; Freimanis, J. *Electrochim. Acta* **1991**, *36*, 1219. Glezer, V.; Turovska, B.; Stradins, J.; Freimanis, J. *Electrochim. Acta* **1990**, *35*, 1933.

(10) Illescas, B.; Martin, N.; Segura, J. L.; Seoane, C.; Orti, E.; Viruela, P. M.; Viruela, R. *J. Org. Chem.* **1995**, *60*, 5643.

(11) Oeriu, I.; Benesch, H. *Bull. Soc. Chim. Biol.* **1962**, *44*, 91. Oeriu, I. *Biokhimiya* **1963**, *28*, 380.

(12) Prescott, B. *J. Med. Chem.* **1969**, *12*, 181.

(13) Silver, R. F.; Holmes, H. L. *Can. J. Chem.* **1968**, *46*, 1859.

(14) Hodnett, E. M.; Wongwiechintana, C.; Dunn, W. J.; Marrs, P. *J. Med. Chem.* **1983**, *26*, 570.

(15) Lopez, J. N. C.; Johnson, A. W.; Grove, J. F.; Bulhoes, M. S. *Cienc. Cult. (Sao Paulo)* **1977**, *29*, 1145.

(16) U.S. Rubber Co., British Patent 862 489, 1959. Takeda Chemical Industry Co. Ltd., Japanese Patent 18 520, 1963. Ube Industries Ltd., Japanese Patent 126 725, 1979. Shell Internationale Research Maatschappij B.V., British Patent 1 314 881, 1973.

(17) Clark, N. G. *Pestic. Sci.* **1985**, *16*, 23.

(18) Krygowski, T. M.; Stępień, B. T. *Chem. Rev.* **2005**, *105*, 3482.

(19) Exner, O.; Böhm, S. *Curr. Org. Chem.* **2006**, *10*, 763.

(20) King-Diáz, B.; Macías-Ruvalcaba, N. A.; Aguilar-Martínez, M.; Calaminici, P.; Köster, A. M.; Gómez-Sandoval, Z.; Reveles, J. U.; Lotina-Hennsen, B. *J. Photochem. Photobiol., B* **2006**, *83*, 105.

(21) Peover, M. E. *Trans. Faraday Soc.* **1962**, *58*, 2370.

(22) Rüssel, C.; Jaenicke, W. *J. Electroanal. Chem.* **1986**, *199*, 139.

(23) Sasaki, K.; Kashimura, T.; Ohura, M.; Ohsaki, Y.; Ohta, N. *J. Electrochem. Soc.* **1990**, *137*, 2437.

(24) Gómez-Sandoval, Z. *σ - π Energy Separation in Density Functional Theory: Implementation and Application*, Ph.D. Thesis, Cinvestav, Mexico-City, 2005.

(25) Jug, K.; Hiberty, P. C.; Shaik, S. *Chem. Rev.* **2001**, *101*, 1477.

(26) Köster, A. M.; Calaminici, P.; Flores-Moreno, R.; Geudtner, G.; Goursot, A.; Heine, T.; Janetzko, F.; Patchkovskii, S.; Reveles, J. U.; Vela, A.; Salahub, D. R. *deMon2k*; The deMon Developers: 2005.

(27) Dirac, P. A. M. *Proc. Cambr. Phil. Soc.* **1930**, *26*, 376.

(28) Vosko, S. H.; Wilk, L.; Nusair, M. *Can. J. Phys.* **1980**, *58*, 1200.

(29) Becke, A. D. *Phys. Rev. A* **1988**, *38*, 3098.

(30) Lee, C.; Yang, W.; Parr, R. G. *Phys. Rev. B* **1988**, *37*, 785.

(31) Godbout, N.; Salahub, D. R.; Andzelm, J.; Wimmer, E. *Can. J. Phys.* **1992**, *70*, 560.

(32) Dunlap, B. I.; Connolly, J. W. D.; Sabin, J. R. *J. Chem. Phys.* **1979**, *71*, 4993.

(33) Reveles, J. U.; Köster, A. M. *J. Comput. Chem.* **2004**, *25*, 1109.

(34) Köster, A. M.; Reveles, J. U.; del Campo, J. M. *J. Chem. Phys.* **2004**, *121*, 3417.

(35) Aguilar-Martínez, M.; Cuevas, G.; Jiménez-Estrada, M.; González, I.; Lotina-Hennsen, B.; Macías-Ruvalcaba, N. *J. Org. Chem.* **1999**, *64*, 3684.

(36) Aguilar-Martínez, M.; Bautista-Martínez, J. A.; Macías-Ruvalcaba, N.; González, I.; Tovar, E.; Marín del Alizal, T.; Collera, O.; Cuevas, G. *J. Org. Chem.* **2001**, *66*, 8349.

(37) van Bolhuis, F.; Kiers, C. *Acta Crystallogr., Sect. B: Struct. Sci.* **1978**, *34*, 1015.

(38) Gaultier, J.; Hauw, C. *Acta Crystallogr.* **1965**, *18*, 179.

(39) Krygowski, T. M.; Cyrański, M. K. *Chem. Rev.* **2001**, *101*, 1385.

(40) Bodwell, G. J.; Bridson, J. N.; Cyrański, M. K.; Kennedy, J. W. J.; Krygowski, T. M.; Mannion, M. R.; Miller, D. O. *J. Org. Chem.* **2003**, *68*, 2089.

(41) Matsunaga, Y.; Miyajima, N.; Togashi, A. *Bull. Chem. Soc. Jpn.* **1977**, *50*, 2234.

(42) Behrens, S.; Köster, A. M.; Jug, K. *J. Org. Chem.* **1994**, *59*, 2546.

(43) González, F.; Aceves, J. M.; Miranda, R.; Gonzáles, I. *J. Electroanal. Chem.* **1991**, *310*, 293.

(44) Frontana, C.; Vázquez-Mayagoitia, A.; Garza, J.; Vargas, R.; González, I. *J. Phys. Chem. A* **2006**, *110*, 9411.

(45) Bard, A. J.; Faulkner, L. R. *Electrochemical Methods*, 2nd ed.; Wiley: New York, 2001.

CT6003356